JCTC Journal of Chemical Theory and Computation

Article

Cite This: J. Chem. Theory Comput. 2018, 14, 4088−4096

pubs.acs.org/JCTC

# Double Precision Is Not Needed for Many-Body Calculations: Emergent Conventional Wisdom

Pavel Pokhilko,[†] Evgeny Epifanovsky,[‡] and Anna I. Krylov*[,†]

[†]Department of Chemistry, University of Southern California, Los Angeles, California 90089-0482, United States

[‡]Q-Chem Inc., 6601 Owens Drive, Suite 105, Pleasanton, California 94588, United States

Supporting Information

**ABSTRACT:** Using single-precision floating-point representation reduces the size of data and computation time by a factor of 2 relative to double precision conventionally used in electronic structure programs. For large-scale calculations, such as those encountered in many-body theories, reduced memory footprint alleviates memory and input/output bottlenecks. Reduced size of data can lead to additional gains due to improved parallel performance on CPUs and various accelerators. However, using single precision can potentially degrade the accuracy of the computed quantities. Here we report an implementation of coupled-cluster and equation-of-motion coupled-cluster methods with single and double excitations in single precision. We consider both standard implementation and one using Cholesky decomposition or resolution-of-the-identity representation of electron-repulsion integrals. Numerical tests illustrate that when single precision is used in correlated calculations, the loss of accuracy is insignificant, and pure single-precision implementation can be used for computing energies, analytic gradients, excited states, and molecular properties. In addition to pure single-precision calculations, our implementation allows one to follow a single-precision calculation by cleanup iterations, fully recovering double-precision results while retaining significant savings.

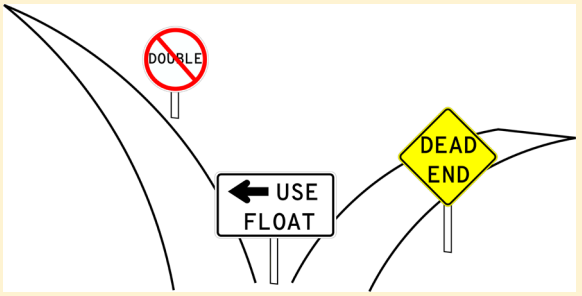




## 1. INTRODUCTION

Quantum chemistry is one of the most demanding fields in terms of computational resources. Standard formulations of many-body theories result in large amounts of data (wave function parameters) and steep computational scaling. For example, storage and floating-point operations requirements of the coupled-cluster method with single and double substitutions (CCSD) scale as $N^4$ and $N^6$ with the system size, respectively.[1] This steep scaling limits the applicability of these highly reliable methods. Large memory footprint, inherent to correlated theories, also creates a hurdle for efficient parallelization and utilization of accelerators (such as graphic processing units, GPUs). In this paper, we present a production-level implementation of CCSD and EOM-CCSD (equation-of-motion CCSD) methods[2−8] and investigate the impact of using reduced precision on the computational efficiency and accuracy of the results.

Chemical accuracy, the minimal accuracy for quantum chemical calculations of thermochemical data, is defined as 1 kcal/mol (which equals 4.2 kJ/mol or $1.593 \times 10^{-3}$ hartree).[9] However, today's standards for chemical kinetics call for a sub-kJ/mol accuracy.[10,11] Typical desired accuracy for excitation and ionization energies is 0.01−0.1 eV. The errors in the calculations arise due to the intrinsic errors of the methods because of approximations made in many-electron and one-electron bases,[1] as well as finite convergence thresholds in employed iterative algorithms. Typically, convergence thresholds are much tighter than the methods' error bars.

The IEEE 754 standard[12,13] defines single- and double-precision floating-point arithmetic, which are almost universally used to represent numbers on most modern CPUs and GPUs. The numbers in this format are represented in the scientific notation

$$(-1)^s b_0.b_1b_2b_3 \ldots b_{p-1}2^E \quad (1)$$

where $s$ is the sign bit, $p$ is the precision of significand, $E$ is the exponent, and bits $b_i$ can take values 0 or 1 (see ref 14). The exponent can take positive and negative values. The format specifies a *biased exponent* $e = E + bias$, allowing to encode exponent $E$ by a non-negative value of $e$. Although the second revision of the standard[13] generalizes base, or *radix*, here we consider only binary formats.[15] The attributes of single- and double-precision floating-point numbers are summarized in Table 1, which shows that a single-precision number takes half the space of a double-precision number and for all practical purposes gives 7 significant figures, whereas double gives 15.

Typical implementations of most *ab initio* methods use double-precision arithmetic. The single-precision format uses half the number of bits of double precision, thereby allowing to store twice as many values. Another benefit is proportionally

Received: April 3, 2018
Published: July 3, 2018




DOI: 10.1021/acs.jctc.8b00321
J. Chem. Theory Comput. 2018, 14, 4088−4096

**Table 1. Summary of Single and Double Floating-Point IEEE 754 Standard**

| | single | double |
|---|---|---|
| total size, bits | 32 | 64 |
| exponent size, bits | 8 | 11 |
| exponent bias | 127 | 1023 |
| sign, bits | 1 | 1 |
| significant (explicit), bits | 23 | 52 |
| decimal precision | $\log_{10}(2^{24}) \approx 7$ | $\log_{10}(2^{53}) \approx 16$ |
| smallest normal number | $2^{-126}$ | $2^{-1022}$ |

faster memory access and disk input/output (in terms of the number of elements per second). This is important in practice because memory speed improves at a slower rate than CPUs. Furthermore, CPU caches can accommodate twice as many floating-point numbers potentially leading to less frequent cache misses. In terms of computational time, single precision gives a 2-fold speedup on CPUs for most modern architectures, and the gains on GPUs can be much larger. Thus, single-precision implementation of quantum-chemistry methods can extend the scope of systems amenable to these treatments, decrease time-to-solution, and reduce energy footprint. Using too much energy and power per calculation is recognized as one of the biggest challenges in high performance computing, and using reduced precision or even an entirely different representation of real numbers has been advocated.[16]

Although early electronic-structure codes, which were very mindful of effective resource usage, utilized mixed precision, today double precision is a *de facto* standard in quantum chemistry and other scientific calculations. However, many algorithms can be redesigned to work in mixed precision, as was recently done in such diverse areas as lattice quantum chromodynamics,[17] molecular dynamics,[18] and general linear algebra algorithms with iterative refinements.[19] The renewed interest in single-precision computations has been largely driven by potential benefits offered by GPUs.[20−26] In quantum chemistry mixed-precision algorithms have been explored in the context of integral calculations[27,28] within Hartree−Fock (HF) and density functional theory (DFT).[20−22,29] The main conclusion from these studies was that pure single precision is not sufficient for integral and HF/DFT calculations and one should only deploy it in a mixed-precision fashion, i.e., such that some operations are performed in single precision and others in double. The utility of single precision has not yet been thoroughly investigated in post-HF calculations. Previous studies[30−32] focused on noniterative methods, such as MP2 and triples correction for CCSD. Single-precision MP2 was tested within resolution-of-the-identity (RI)[30] and Cholesky decomposition (CD)[31] schemes. These studies have shown that commonly used RI bases and CD thresholds ($10^{-2}$−$10^{-3}$) yield much larger errors in total energies than the errors due to using single-precision arithmetic. Within coupled-cluster theory, single-precision algorithms were analyzed within CCD[23] and perturbative triples, (T), correction[32] calculations. GPU implementation of CCD[23] in single precision showed that the numerical error is $10^{-5}$−$10^{-6}$ hartree. Numerical analysis of the (T) correction for CCSD[32] has shown that the result is stable with respect to numerical noise, justifying a single-precision implementation.

Despite these encouraging findings, the extent of applicability of single precision in many-body theories is not fully understood. There are several open questions:

1. Does numerical error accumulate in iterative procedures such as those used to solve CCSD and EOM equations?
2. What is the impact of using single precision on molecular properties and excited states?
3. Can one reliably compute analytic nuclear gradients and optimize structures within pure single precision?

In this paper, we show that using pure single-precision implementation of post-HF methods is sufficient for most quantum-chemistry applications. Thus, one can reap the benefits of reduced costs without invoking more sophisticated mixed-precision algorithms, which can be reserved for more exotic situations when much higher numeric accuracy is desired.

As a standard practice in quantum chemistry, typical numerical convergence thresholds are tight enough to not affect the resulting accuracy. For example, Q-Chem's default CCSD convergence criteria are $10^{-6}$ hartree for energies and $10^{-4}$ for amplitudes;[33] Molpro uses $10^{-6}$ hartree for energies and $10^{-5}$ for amplitudes.[34] Some packages use a single threshold, for example, GAMESS uses $10^{-7}$ for amplitudes[35] and ORCA uses $10^{-5}$−$10^{-6}$ hartree for energies. Thus, it appears that 7 decimal digits is sufficient for correlation energy

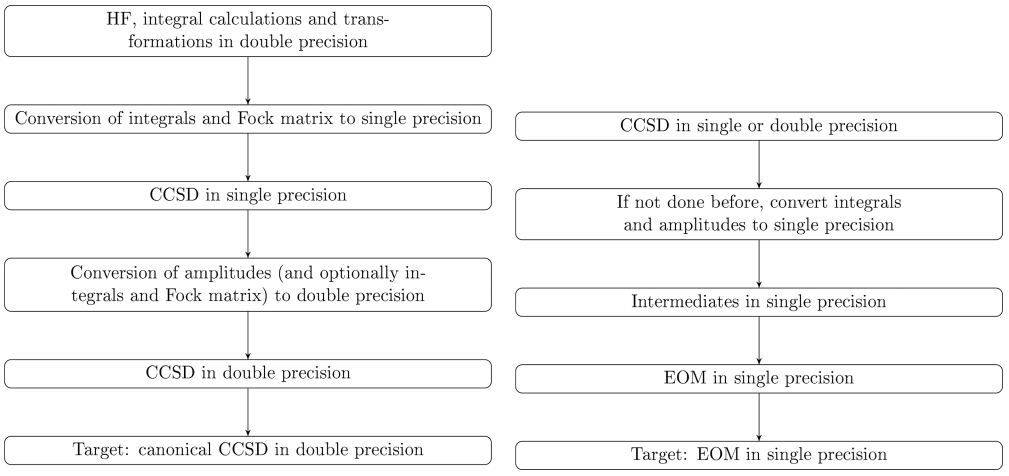


**Figure 1.** Left: Implemented CCSD algorithm. Cleanup iterations in double precision are optional. Right: EOM algorithm.



DOI: 10.1021/acs.jctc.8b00321
J. Chem. Theory Comput. 2018, 14, 4088−4096

(we note that $10^{-7}$ hartree is 3 orders of magnitude tighter that chemical accuracy).

In this paper, we describe a general implementation of CC/EOM-CC methods that allows users to perform calculations in either single or double precision. We implemented both the standard variant and one using CD and RI representation of electron-repulsion integrals. In addition, our implementation allows one to follow up a single-precision calculation with cleanup iterations, in which the full double-precision accuracy can be recovered.[23] The code is based on the libtensor[36] and libxm[37] libraries for many-body electronic structure calculations. The production-level code is implemented in the Q-Chem electronic structure package.[38,39]

## 2. ALGORITHMS AND IMPLEMENTATION DETAILS

Libtensor[36] was developed to provide a high-level interface for tensor operations and to deliver efficient performance. The library has been used to implement a large number of CC,[2−4] EOM-CC,[6−8,40] and ADC (algebraic diagrammatic construction)[41] methods for calculating energies, nuclear gradients, and properties in Q-Chem. Libtensor supports tensor symmetries, block-sparsity, several contraction algorithms, different BLAS implementations, and several computational backends.[37,42] We extended the libtensor library to incorporate single-precision operations by generalizing all tensor operations for the general element type (Figure S1 in the SI gives an example of the code). The code is available in the original repository on GitHub.[43] The numerical tests presented in this paper were performed with a developer version of Q-Chem and the modified libtensor, compiled with the GCC-6.4.0 compiler using the '-O3' optimization flag and linked against the Intel MKL library (2017.0 version).

Figure 1 shows an overview of the CCSD and EOM-CCSD workflows. In our implementation, we compute all integrals and solve HF equations in double precision; the integral transformation step is also performed in double precision. We then convert the tensors (integrals) to single precision and perform all tensor operations (contractions, additions, etc.) in the CCSD/EOM-CCSD calculations using single precision. In the RI/CD variants, we also employ the single-precision algorithm at the CCSD step. Once the CCSD equations converge in single precision, the procedure can switch to double precision to perform cleanup iterations to recover the double-precision result. We follow the same strategy for Λ-amplitudes. We also implemented single-precision calculations of various density matrices needed for property and nuclear gradient calculations.

The EOM workflow entails solving the CCSD equations and evaluating the similarity-transformed Hamiltonian ($\bar{H}$) intermediates followed by the computation of EOM energies and amplitudes by iterative diagonalization of the similarity-transformed Hamiltonian using the Davidson algorithm. We extended the routines[44] that compute the intermediates and σ-vectors (products of the similarity-transformed Hamiltonian acting on EOM trial states) for EOM-IP/EA/SF/EE-CCSD to support calculations in single precision.

It is expected that using single precision provides a speedup factor of 2 on CPUs (this estimate does not take into account reduced I/O, which can speed the calculation even further if single-precision tensors fit in RAM, while double-precision tensors do not). If the single-precision calculation is followed up by cleanup iterations to recover double-precision accuracy, the theoretical estimate for the overall speedup is

$$\text{Theor. speedup} = \frac{N_{dp}}{0.5 \cdot N_{sp} + N_{cleanup}} \quad (2)$$

where $N_{dp}$ and $N_{sp}$ are the number of iterations in double and single precisions, and $N_{cleanup}$ is the number of cleanup iterations in double precision.

## 3. COMPUTATIONAL DETAILS

Benchmark calculations of water clusters were performed on a Dell server with four 8-core Intel Xeon E5-4640 processors using 4 threads. We used 4 threads to avoid bias for small jobs, which cannot be effectively parallelized using too many threads. All other calculations were performed on Dell servers with four 8-core Intel Xeon E5-4640, two 8-core Intel Xeon E5-2690, or two 10-core Intel Xeon E5-2689 v4 processors with the best settings, i.e., utilizing all cores and using maximum available memory. The benchmark set comprises diverse types of electronic structure, including water clusters of increasing size, the uracil molecule, the formaldehyde molecule, oxygen-ethylene adduct ($C_2H_4O$), a nucleobase trimer (ATT, adenine-thymine-thymine), an aromatic diradical ($C_6H_5N$), the benzene molecule, and the G2 set[45] containing 148 molecules. To assess numerical errors in very large systems, we used the taxol molecule (110 atoms, 446 electrons).

We tested basis sets of the double-, triple-, quadruple-, and pentuple-zeta quality, with and without diffuse functions, and including polarized-core variants. Frozen core was used for all calculations, except water dimer and formaldehyde calculations with cc-pCVXZ basis sets. All Cartesian geometries are given in the Supporting Information (SI). The structure of taxol is from ref 31.

Convergence thresholds for CCSD equations are summarized in Table 2. Since single precision provides ∼7 decimal digits of precision, the tightest threshold of convergence for energy in single precision is $10^{-7}$ hartree (assuming correlation energies of ∼1 hartree). By numerical experimentation we found that single-precision iterations converge smoothly with the energy threshold of $10^{-5}$−$10^{-6}$ hartree; therefore, we used this threshold for the single-precision part of the calculation in most cases. In the double-precision calculations, we used default convergence except for the benzene benchmark. In properties calculations, we used the same convergence criteria

**Table 2. Convergence Thresholds for CCSD Calculations[a]**

| system | $E$, sp, hartree | $T$, sp | $E$, dp, hartree | $T$, dp |
|---|---|---|---|---|
| water clusters | $10^{-5}$ | $10^{-3}$ | $10^{-6}$ | $10^{-4}$ |
| water dimer (dipole moment run) | $10^{-6}$ | $10^{-4}$ | $10^{-6}$ | $10^{-4}$ |
| uracil | $10^{-6}$ | $10^{-4}$ | $10^{-6}$ | $10^{-4}$ |
| $CH_2O$ | $10^{-6}$ | $10^{-4}$ | $10^{-6}$ | $10^{-4}$ |
| $C_2H_4O$ | $10^{-6}$ | $10^{-4}$ | $10^{-6}$ | $10^{-4}$ |
| ATT | $10^{-6}$ | $10^{-4}$ | $10^{-6}$ | $10^{-4}$ |
| G2 set, pure sp or dp | $10^{-6}$ | $10^{-4}$ | $10^{-6}$ | $10^{-4}$ |
| G2 set, sp with cleanup | $10^{-5}$ | $10^{-3}$ | $10^{-6}$ | $10^{-4}$ |
| G2 set, sp with energy in dp | $10^{-5}$ | $10^{-3}$ | | |
| G2 set, pure sp or dp, optimization | $10^{-7}$ | $10^{-5}$ | $10^{-7}$ | $10^{-5}$ |
| $C_6H_5N$ | $10^{-6}$ | $10^{-4}$ | $10^{-6}$ | $10^{-4}$ |
| benzene | $10^{-10}$ | $10^{-9}$ | $10^{-7}$ | $10^{-5}$ |

[a]Convergence for Λ equations is the same as for the $T$ amplitudes.



DOI: 10.1021/acs.jctc.8b00321
J. Chem. Theory Comput. 2018, 14, 4088−4096

Table 3. CCSD/cc-pVDZ Total Energies of Water Clusters[a]

| cluster size | $E_{sp}$, au | $E_{sp+dp}$, au | $E_{dp}$, au | $\Delta_{dp,sp}$, J/mol |
|---|---|---|---|---|
| 2 | −152.48710832 | −152.48710752 | −152.48710767 | 1.7 |
| 3 | −228.74911206 | −228.74911017 | −228.74911059 | 3.9 |
| 4 | −305.00868540 | −305.00868416 | −305.00868472 | 1.8 |
| 5 | −381.26858576 | −381.26858599 | −381.26858585 | −0.2 |
| 6 | −457.51949116 | −457.51949130 | −457.51949145 | −0.8 |
| 7 | −533.78980571 | −533.78980623 | −533.78980640 | −1.8 |

[a]Differences between single- and double-precision energies are shown in the last column.

Table 4. CD-CCSD/cc-pVDZ Total Energies of Water Clusters[a]

| cluster size | $E_{sp}$, au | $E_{sp+dp}$, au | $E_{dp}$, au | $\Delta_{dp,sp}$, J/mol |
|---|---|---|---|---|
| 2 | −152.48713650 | −152.48713571 | −152.48713586 | 1.7 |
| 3 | −228.74916915 | −228.74916737 | −228.74916779 | 3.6 |
| 4 | −305.00875903 | −305.00875662 | −305.00875717 | 4.9 |
| 5 | −381.26864546 | −381.26864554 | −381.26864540 | 0.2 |
| 6 | −457.51960841 | −457.51960843 | −457.51960858 | −0.4 |
| 7 | −533.78994271 | −533.78994226 | −533.78994243 | 0.7 |

[a]Cholesky threshold of $10^{-3}$ was used. Differences between single- and double-precision energies are shown in the last column.

for $T$ and $\Lambda$ amplitudes. Unrelaxed one-particle density matrices used in dipole moment calculations were computed in double and single precision from respective double- and single-precision intermediates and amplitudes. In all EOM calculations a $10^{-5}$ convergence threshold for EOM amplitudes[46] was used in the Davidson procedure. For geometry optimization (benzene) and finite-difference frequency analysis, much tighter convergence criteria were used: $10^{-10}$ for energies, $10^{-9}$ for $T$, and $\Lambda$ amplitudes in double precision; $10^{-7}$ for energies, $10^{-5}$ for $T$, and $\Lambda$ amplitudes in single precision. The criteria of convergence in geometry optimization were the same for the double- and single-precision calculations: $2 \times 10^{-5}$ au for the maximum component of the gradient, $5 \times 10^{-5}$ au for the maximum atomic displacement, and $1 \times 10^{-7}$ au for energy. Such tight criteria would reveal how different the "best" geometry from single-precision calculation is from the geometry from the "best" double-precision calculation.

For geometry optimization of the systems from the G2 set, we used default Q-Chem convergence criteria on gradient, displacement, and energy change, $10^{-7}$ au for energies, $10^{-5}$ for $T$, and $\Lambda$ amplitudes for both precisions, which are the default for double precision.

## 4. RESULTS AND DISCUSSION

**4.1. Accuracy of Ground-State Energies and Properties.** We found that the CC amplitude convergence rate is not affected by using single precision and that the number of CCSD iterations in calculations with single-precision CCSD followed by cleanup iterations is the same as in reference double-precision calculations. The typical output of a single-precision calculation with cleanup iterations is shown in the SI (Figure S2).

Table 3 and Table 4 show the results for water clusters. Pure single-precision calculations (without cleanup iterations) do not introduce significant numerical errors in total energies, i.e. the typical difference between single- and double-precision energies is only several J/mol, which is 3 orders of magnitude below chemical accuracy. Moreover, double-precision numerical accuracy is fully recovered when cleanup iterations are performed. The single-precision calculation is twice as fast than the double-precision one. In calculations with cleanup iterations, observed speedup quickly approaches the theoretical maximum (about 1.6, for these parameters) with the increasing number of water molecules (see Figure 2). For all water clusters only two cleanup iterations were needed to converge calculations within the convergence criteria (Table 2). At the first cleanup iteration the change in energy is small, but the net change of amplitudes is large (this is illustrated in Figure S2 in the SI). If only energy criterion of convergence is used, only one cleanup iteration is necessary in most cases. The explanation of the net change in the amplitudes is simple: switching to double-precision changes all amplitudes by a small amount (that is why it is "cleanup") but because the number of amplitudes is large, the net change is large (this is also confirmed by the increase of this net change with the size of the cluster). The second cleanup iteration does not include change of precision, and the calculation quickly converges. We observed similar performance and accuracy for RI/CD-CCSD calculations of these clusters.

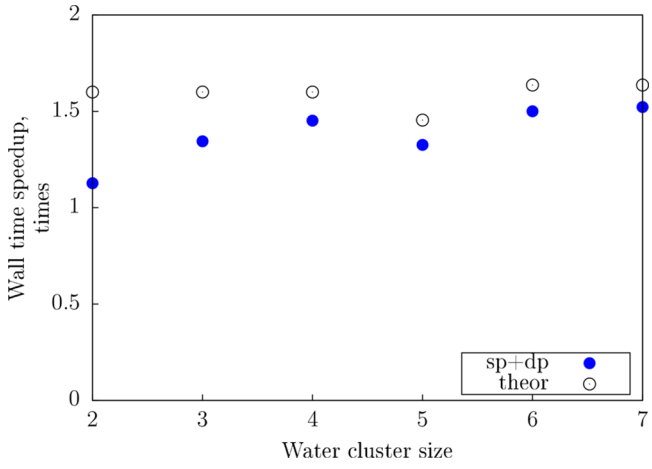


**Figure 2.** Wall time speedup for SP scheme with cleanup iterations for the CCSD/cc-pVDZ energy calculations of water clusters. Theoretical estimate is given by eq 2.



DOI: 10.1021/acs.jctc.8b00321
J. Chem. Theory Comput. 2018, 14, 4088−4096

Table 5. CCSD Total Energies (Hartree) and Dipole Moments ($\mu$, au) of Uracil, Water Dimer, Formaldehyde, and Ethylene-Oxygen Adduct in Various Basis Sets[a]

| | $E_{sp}$, au | $E_{dp}$, au | $\Delta_{dp,sp}$, J/mol | $\mu_{sp}$, au[b] | $\mu_{dp}$, au[c] |
|---|---|---|---|---|---|
| uracil/basis set | | | | | |
| cc-pVDZ | −413.72139806 | −413.72139812 | −0.2 | 1.550917 | 1.550917 |
| cc-pVTZ | −414.10170402 | −414.10170403 | 0.0 | 1.643366 | 1.643366 |
| aug-cc-pVTZ | −414.13153216 | −414.13153108 | 2.8 | 1.689405 | 1.689405 |
| cc-pVQZ | −414.22039427 | −414.22039569 | −3.7 | 1.683603 | 1.683603 |
| $(H_2O)_2$/basis set[d] | | | | | |
| cc-pCVTZ | −152.77124280 | −152.77124301 | −0.6 | 0.758536 | 0.758536 |
| cc-pCVQZ | −152.83005083 | −152.83005083 | 0 | 0.746618 | 0.746618 |
| cc-pCV5Z | −152.84874263 | −152.84874291 | −0.7 | 0.740770 | 0.740770 |
| $CH_2O$/basis set[d] | | | | | |
| cc-pCVTZ | −114.42374047 | −114.42374037 | 0.3 | 0.912793 | 0.912793 |
| cc-pCVQZ | −114.46445277 | −114.46445284 | −0.2 | 0.946294 | 0.946294 |
| cc-pCV5Z | −114.47693774 | −114.47693771 | 0.1 | 0.961034 | 0.961035 |
| $C_2H_4O$ ($T_1$)/basis set | | | | | |
| cc-pVDZ | −153.28012439 | −153.28012442 | −0.1 | 0.713475 | 0.713475 |
| cc-pVTZ | −153.42725145 | −153.42725167 | −0.6 | 0.752959 | 0.752959 |
| cc-pVQZ | −153.47046520 | −153.47046539 | −0.5 | 0.778434 | 0.778434 |
| $C_2H_4O$ ($S_0$)/basis set | | | | | |
| cc-pVDZ | −153.24187533 | −153.24187486 | 1.2 | 0.930752 | 0.930749 |
| cc-pVTZ | −153.39033087 | −153.39033115 | −0.7 | 1.155325 | 1.155318 |
| cc-pVQZ | −153.43514375 | −153.43514491 | −3.0 | 1.272352 | 1.272339 |

[a]Convergence thresholds for single and double precision are the same (see Table 2). [b]Equations for T and Λ equations are solved in single precision; intermediates and unrelaxed density matrices are evaluated in single precision. [c]Equations for T and Λ equations are solved in double precision; intermediates and unrelaxed density matrices are evaluated in double precision. [d]All electron were active in the cc-pCVTZ, cc-pCVQZ, and cc-pCV5Z calculations.

To test whether numerical errors increase with system size, we compared single- and double-precision CCSD for an adenine-thymine-thymine system (ATT) and found that the difference between single- and double-precision total energies is 15 J/mol (again, full double-precision accuracy can be recovered with one or two cleanup iterations). As an example of an even larger system, we carried out RI-MP2/cc-pVDZ calculations of taxol with double-precision amplitudes and with the amplitudes converted to single precision. The resulting single- and double-precision energies are −2918.93641306 and −2918.93643602 hartree, respectively. Although the error due to single precision is larger (60 J/mol), it is still well below 1 kJ/mol. The MP2 correlation energy is −8.9646559≈−10 hartree, thus, the tightest convergence criterion by energy for a corresponding single-precision CCSD calculation would be $10^{-6}$ hartree.

We investigated basis set effects on the error due to single precision by using uracil, formaldehyde, and the water dimer. Table 5 presents total energies and dipole moments for all species. The results show that the errors in energies are negligible and that the differences in dipole moments computed in single and double precision are less than the number of digits printed in the output. Increasing the basis set from cc-pVDZ to cc-pVTZ and aug-cc-pVTZ does not increase the errors. The results for formaldehyde and water dimer and for which a larger set of basis sets was used (up to cc-pCV5Z) follow the same trend, and the magnitude of errors due to single precision does not increase.

In order to meaningfully compare the differences between single and double precision, one should keep in mind that in these calculations the energy threshold for CCSD convergence was $10^{-6}$ hartree ≈ 2.6 J/mol. Within this threshold, the error of the calculations with the cleanup iterations is the same as in the single-precision calculation. Interestingly, calculation of double-precision energies from single-precision amplitudes gives larger errors, which can be explained by the convergence criteria used: the amplitudes are underoptimized in comparison with the amplitudes, used for other calculations (shown in Table 2).

To test the behavior of the single-precision algorithm in strongly correlated systems, we considered ethylene-oxygen adduct, an important intermediate in the reaction of atomic oxygen with ethylene. This molecule can be described as an oxyrane ring with one broken C−O bond, which results in strong diradical character. This is a somewhat artificial example, because standard CCSD is expected to perform poorly in strongly correlated systems. These types of electronic structure should be described by, for example, spin-flip[47,48] or double ionization potential[49] variants of EOM-CC. We performed CCSD calculations for the singlet and triplet states. The triplet solution is well-behaved, e.g., $\|T_1\|^2 = 0.0115$ and $\|T_2\|^2 = 0.1724$ in the cc-pVQZ basis, and for either precision CCSD converges in 10, 11, and 11 iterations with cc-pVDZ, cc-pVTZ, and cc-pVQZ, respectively. As expected, the description of the singlet state is problematic ($\|T_1\|^2 = 1.1296$ and $\|T_2\|^2 = 0.5336$ in cc-pVQZ). Such large $T_1$ amplitudes are due to open-shell character of the state, which renders a closed-shell determinant to be a poor quality zero-order wave function. This is a likely cause of the observed slow convergence of CCSD (31−35 iterations for $T$ and 51−56 iterations for Λ), yet the number of iterations in single and double precision was the same, except for cc-pVQZ where the number of iterations in single and double precision differed by one. Importantly, the errors of pure single-precision CCSD


DOI: 10.1021/acs.jctc.8b00321
J. Chem. Theory Comput. 2018, 14, 4088−4096

total energies are of the same magnitude as in the previous examples.

To confirm that these observations hold for other systems, we compared the CCSD total energies computed in single and double precision for the G2 set[45] using the 6-31G(d), cc-pVDZ, cc-pVTZ, and cc-pVQZ basis sets. In addition, we compared single-precision results with those obtained with cleanup iterations, as well as a calculation in which energy is computed in double precision using double-precision integrals and single-precision amplitudes. The results are summarized in Table 6. As one can see, the MAD (mean absolute deviation) in single-precision calculations is less than 4 J/mol. The MADs, STDs (standard deviation, unbiased estimate), and maximum errors in cc-pVQZ basis are only slightly larger than in cc-pVDZ.

**Table 6. Mean Average Deviation (MAD) and Standard Deviation (STD), J/mol, from Reference Double-Precision CCSD Total Energies for the G2 Set**

| | sp | | sp with dp energy | | sp with cleanup | |
|---|---|---|---|---|---|---|
| basis | MAD | STD | MAD | STD | MAD | STD |
| 6-31G(d) | 0.12 | 0.2 | 3.7 | 6.6 | 1.5 | 1.4 |
| cc-pVDZ | 0.15 | 0.2 | 3.6 | 6.7 | 1.4 | 1.4 |
| cc-pVTZ | 0.30 | 0.5 | 3.4 | 5.3 | 1.5 | 1.4 |
| cc-pVQZ | 0.68 | 0.9 | 3.7 | 5.0 | 1.6 | 1.5 |

**4.2. Accuracy of Target-State Energies in EOM-CCSD.** To test the accuracy of single-precision calculations of excited states, we carried out EOM-EE-CCSD calculations for uracil (Table 7) and EOM-SF-CCSD calculations for $C_6H_5N$ (Table 8). We considered different types of states: singlets and triplets, states with different symmetry (symmetric and antisymmetric with respect to the symmetry plane), closed-shell and open-shell types, and valence and Rydberg states. In all cases, the difference between total energies computed in double and single precision does not exceed 3 J/mol ($3 \times 10^{-5}$ eV), which is much smaller than the intrinsic error bars of EOM-CCSD (0.1−0.3 eV). This result is comparable to the differences in the CCSD total energies. The respective excitation energies are the same within at least 4 decimal places.

**4.3. Accuracy of Gradient Evaluation in Single Precision.** To test how the choice of precision affects the accuracy of the nuclear gradient and the resulting optimized structures, we first optimized the benzene molecule at the CCSD/cc-pVDZ level of theory using tight convergence criteria. In these calculations, density matrices were computed in the respective precisions; orbital response was computed in double precision. Geometry optimization was performed by gradient optimization (gradient was evaluated analytically). Starting from the same initial geometry (MP2/cc-pVDZ optimized structure), both optimizations converged in 6 iterations (single precision run converged by gradient and displacement). The resulting geometries (given in section 2 of the SI) are nearly identical, with mean absolute error

**Table 7. EOM-EE-CCSD Total Energies (in au) of Excited Singlet and Triplet States of Uracil in Various Basis Sets[a]**

| singlets | 1A′ | 2A′ | 1A″ | 2A″ |
|---|---|---|---|---|
| basis set | | | | |
| cc-pVDZ | −413.50624322 | −413.46584035 | −413.52849406 | −413.47629005 |
| | −413.50624315 | −413.46584026 | −413.52849409 | −413.47628997 |
| | −413.50624328 | −413.46584041 | −413.52849406 | −413.47629005 |
| | $-7 \times 10^{-8}$ | $-9 \times 10^{-8}$ | $3 \times 10^{-8}$ | $-8 \times 10^{-8}$ |
| cc-pVTZ | −413.89150482 | −413.84840838 | −413.90876266 | −413.85792039 |
| | −413.89150498 | −413.84840792 | −413.90876251 | −413.85792058 |
| | −413.89150563 | −413.84840854 | −413.90876290 | −413.85792110 |
| | $1.6 \times 10^{-7}$ | $-4.6 \times 10^{-7}$ | $-1.5 \times 10^{-7}$ | $1.9 \times 10^{-7}$ |
| aug-cc-pVTZ | −413.92599740 | −413.88373275 | −413.94000534 | −413.90496469 |
| | −413.92599743 | −413.88373272 | −413.94000543 | −413.90496414 |
| | −413.92599918 | −413.88373397 | −413.94000635 | −413.90496581 |
| | $3 \times 10^{-8}$ | $-3 \times 10^{-8}$ | $9 \times 10^{-8}$ | $-5.5 \times 10^{-7}$ |
| triplets | 1A′ | 2A′ | 1A″ | 2A″ |
| basis set | | | | |
| cc-pVDZ | −413.57714822 | −413.51667861 | −413.53936723 | −413.48574474 |
| | −413.57714817 | −413.51667858 | −413.53936718 | −413.48574485 |
| | −413.57714827 | −413.51667865 | −413.53936732 | −413.48574489 |
| | $-5 \times 10^{-8}$ | $-3 \times 10^{-8}$ | $-5 \times 10^{-8}$ | $1.1 \times 10^{-7}$ |
| cc-pVTZ | −413.95932894 | −413.89779284 | −413.91902233 | −413.86657196 |
| | −413.95932869 | −413.89779281 | −413.91902181 | −413.86657206 |
| | −413.95932945 | −413.89779339 | −413.91902247 | −413.86657255 |
| | $-2.5 \times 10^{-7}$ | $-3 \times 10^{-8}$ | $-5.2 \times 10^{-7}$ | $1.0 \times 10^{-7}$ |
| aug-cc-pVTZ | −413.99008713 | −413.92935022 | −413.94969790 | −413.90754309 |
| | −413.99008666 | −413.92935024 | −413.94969820 | −413.90754252 |
| | −413.99008779 | −413.92935158 | −413.94969912 | −413.90754422 |
| | $-4.7 \times 10^{-7}$ | $2 \times 10^{-8}$ | $3.0 \times 10^{-7}$ | $-5.7 \times 10^{-7}$ |

[a]In each cell the first number is obtained from double-precision calculation, the second number is obtained from single-precision EOM calculation from double-precision reference, and the third number is single-precision EOM from single-precision reference. The fourth number is the difference between double- and single-precision energies (with double-precision reference).



DOI: 10.1021/acs.jctc.8b00321
J. Chem. Theory Comput. 2018, 14, 4088−4096

Table 8. EOM-SF-CCSD Total Energies (in au) of Several Electronic States of $C_6H_5N$ in Various Basis Sets[a]

| basis set | $1A_2$ | $2A_2$ | $1A_1$ | $2A_1$ |
|---|---|---|---|---|
| cc-pVDZ | −285.46570954 | −285.42658952 | −285.40655223 | −285.37250140 |
| | −285.46570956 | −285.42658954 | −285.40655224 | −285.37250139 |
| | $2 \times 10^{-8}$ | $2 \times 10^{-8}$ | $1 \times 10^{-8}$ | $-1 \times 10^{-9}$ |
| cc-pVTZ | −285.79837285 | −285.76114321 | −285.74329035 | −285.70728705 |
| | −285.79837303 | −285.76114343 | −285.74328950 | −285.70728629 |
| | $1.8 \times 10^{-7}$ | $2.2 \times 10^{-7}$ | $-8.5 \times 10^{-7}$ | $-7.6 \times 10^{-7}$ |

[a]Symmetry labels refer to state symmetries. In each cell the first number is from double-precision calculation, the second number is from single-precision EOM calculation, and the third number is the difference between double- and single-precision energies. CCSD equations were solved in double precision in all cases.

(computed for nonzero Cartesian coordinates) of $1.9 \times 10^{-9}$ Å.

To confirm this result for a larger set of systems, we carried out geometry optimizations of the G2 set with cc-pVTZ in both precisions. The set includes 712 bonds. The bond lengths were extracted from the Cartesian geometries using the *Openbabel* package.[50] The errors with respect to double precision are small: MAD is $6.7 \times 10^{-5}$ Å, STD is $2.1 \times 10^{-4}$ Å, and maximal absolute deviation is $2.5 \times 10^{-3}$ Å. Although the standard deviation is larger in comparison with the benzene result, we note that the shape of statistical distribution is very narrow with a sharp spike at zero. An error interval ($-10^{-7}$ Å, $10^{-7}$ Å) contains about a half of the total number of bonds, explaining the discrepancy with standard deviation. To put these differences in context, we note that the CCSD/cc-pVTZ MAD relative to the experimental bond lengths is about 0.64 pm = 0.006 Å,[1] which is by 2 orders of magnitude larger than the MAD due to using single precision.

**4.4. Accuracy of Finite-Difference Frequencies.** To investigate whether finite-difference calculations of frequencies (using analytic gradients) can be carried out in single precision, we computed the frequencies and normal modes for benzene at the respective optimized geometries with the same convergence criteria as used for geometry optimizations with the step size of 0.001 Å. The resulting frequencies (given in section 3 of the SI) are very different: real and imaginary frequencies of ∼15,000 $cm^{-1}$ occur along with several imaginary frequencies. Thus, not surprisingly, single precision can cause problems in finite-difference calculations. However, finite-difference calculations using single-precision calculation with the double-precision cleanup iterations fully recover double-precision frequencies, while affording ∼×1.3 speedup of the calculation.

We note that finite difference derivative evaluation is always a balance between the size of the step and the accuracy due to finite numerical precision. The default step size of 0.001 Å requires energies converged to $10^{-9}$ or so. Thus, an erratic behavior of single-precision finite-difference calculations can be remedied by using a larger step size. The calculation with 0.01 Å displacements yielded almost identical frequencies in double and single precision with maximal difference in frequencies of 0.64 $cm^{-1}$. The MAD between double-precision frequencies computed with 0.001 and 0.01 Å steps is 0.21 $cm^{-1}$.

## 5. CONCLUSION

In this contribution, we report single- and mixed-precision implementation of the CCSD and EOM-CCSD energies, analytic gradients, and properties. Using single-precision results in reduced memory footprint, considerable computation speedup, and reduced energy-to-solution. That is, single-precision calculations use half the memory (or disk) space and produce a speedup factor of 2 on CPUs. The main focus of this paper was on assessing the impact on accuracy of the resulting energies and properties in post-HF calculations, in particular in iterative schemes. The results show that the rate of error accumulation in single precision is sufficiently slow, and overall single precision introduces negligible errors for total energies, excitation energies, forces, and properties. Moreover, single precision can be used in geometry optimizations with analytical gradients. Thus, we conclude that for most types of calculations, straight single-precision implementation of post-HF methods can be used, and one can reap the benefits of reduced costs without invoking more sophisticated mixed-precision algorithms, which can be reserved for more exotic situations when much higher numeric accuracy is desired. On the basis of these results, the default precision of the CC/EOM-CC calculations will be changed to single precision in a future release. If tight convergence is desired (e.g., in finite-difference calculations), single precision can be used to speedup iterations in the beginning, converging to the single-precision result first and continuing in double precision. In most cases the total number of iterations is not affected, and the speedup is close to the theoretical estimate.

## ■ ASSOCIATED CONTENT

### Supporting Information

The Supporting Information is available free of charge on the ACS Publications website at DOI: 10.1021/acs.jctc.8b00321.

Details of computer implementation, relevant Cartesian geometries, optimized structures, and frequencies and normal modes (PDF)

## ■ AUTHOR INFORMATION


### Corresponding Author

*E-mail: krylov@usc.edu.

### ORCID

Pavel Pokhilko: 0000-0001-5754-9836

Anna I. Krylov: 0000-0001-6788-5016



### Funding

This work was supported by the U.S. Air Force of Scientific Research (AFOSR) under contractor number FA9550-16-1-0051. P.P. is a grateful recipient of the internship fellowship from Q-Chem, Inc.


### Notes

The authors declare the following competing financial interest(s): A.I.K. is a part owner and board member of Q-Chem, Inc.



DOI: 10.1021/acs.jctc.8b00321
J. Chem. Theory Comput. 2018, 14, 4088−4096

## ■ ACKNOWLEDGMENTS

The authors acknowledge Dr. Jeff R. Hammond who presented the basic idea at the MolSSI workshop in Asilomar (May 2017). The MolSSI initiative is supported by the National Science Foundation (molssi.org).

## ■ REFERENCES

(1) Helgaker, T.; Jørgensen, P.; Olsen, J. *Molecular Electronic Structure Theory*; Wiley & Sons: 2000 DOI: 10.1002/9781119019572.
(2) Bartlett, R. J.; Shavitt, I. *Many-Body Methods in Chemistry and Physics: MBPT and Coupled-Cluster Theory*; Cambridge University Press, 2009.
(3) Bartlett, R. J. The Coupled-Cluster Revolution. *Mol. Phys.* **2010**, *108*, 2905−2920.
(4) Bartlett, R. J. In *Theory and Applications of Computational Chemistry*; Dykstra, C., Frenking, G., Scuseria, G., Eds.; Elsevier: 2005.
(5) Bartlett, R. J. To Multireference or Not to Multireference: That Is the Question? *Int. J. Mol. Sci.* **2002**, *3*, 579−603.
(6) Krylov, A. I. Equation-of-Motion Coupled-Cluster Methods for Open-Shell and Electronically Excited Species: The Hitchhiker's Guide to Fock Space. *Annu. Rev. Phys. Chem.* **2008**, *59*, 433−462.
(7) Sneskov, K.; Christiansen, O. Excited State Coupled Cluster Methods. *WIREs Comput. Mol. Sci.* **2012**, *2*, 566−584.
(8) Bartlett, R. J. Coupled-Cluster Theory and Its Equation-of-Motion Extensions. *WIREs Comput. Mol. Sci.* **2012**, *2*, 126−138.
(9) Pople, J. A. Nobel Lecture: Quantum Chemical Models. *Rev. Mod. Phys.* **1999**, *71*, 1267−1274.
(10) Ruscic, B.; Pinzon, R. E.; von Laszewski, G.; Kodeboyina, D.; Burcat, A.; Leahy, D.; Montoy, D.; Wagner, A. F. Active Thermochemical Tables: Thermochemistry for the 21st Century. *J. Phys.: Conf. Ser.* **2005**, *16*, 561.
(11) Tajti, A.; Szalay, P. G.; Császár, A. G.; Kállay, M.; Gauss, J.; Valeev, E. F.; Flowers, B. A.; Vázquez, J.; Stanton, J. F. HEAT: High Accuracy Extrapolated Ab Initio Thermochemistry. *J. Chem. Phys.* **2004**, *121*, 11599−11613.
(12) *IEEE Standard for Binary Floating-Point Arithmetic*; ANSI/IEEE Std 754-1985, 1985; DOI: 10.1109/IEEESTD.1985.82928.
(13) *IEEE Standard for Floating-Point Arithmetic - Redline*; IEEE Std 754-2008 - Redline, 1985; DOI: 10.1109/IEEESTD.2008.5976968.
(14) Although $b_0$ value is implicit and encoded by the exponent, one should consider both implicitly and explicitly stored bits when discussing decimal precision shown in Table 1.
(15) The number is called *normal* if $b_0$ is 1 and subnormal otherwise. Subnormal numbers fill the gap between the smallest positive normal number and zero.
(16) Gustafson, G. J. *Right-Sizing Precision: Unleashed Computing: The Need to Right-Size Precision to Save Energy, Bandwidth, Storage, and Electrical Power*; 2015; Presentation from web archive.https://web.archive.org/web/20160606203112/http://www.johngustafson.net/presentations/Right-SizingPrecision1.pdf (accessed July 12, 2018).
(17) Clark, M. A.; Babich, R.; Barros, K.; Brower, R. C.; Rebbi, C. Solving Lattice QCD Systems of Equations Using Mixed Precision Solvers on GPUs. *Comput. Phys. Commun.* **2010**, *181*, 1517−1528.
(18) Le Grand, S. L.; Götz, A. W.; Walker, R. C. SPFP: Speed Without Compromise − a Mixed Precision Model for GPU Accelerated Molecular Dynamics Simulations. *Comput. Phys. Commun.* **2013**, *184*, 374−380.
(19) Baboulin, M.; Buttari, A.; Dongarra, J.; Kurzak, J.; Langou, J.; Langou, J.; Luszczek, P.; Tomov, S. Accelerating Scientific Computations with Mixed Precision Algorithms. *Comput. Phys. Commun.* **2009**, *180*, 2526−2533. 40 YEARS OF CPC: A celebratory issue focused on quality software for high performance, grid and novel computing architectures.
(20) Ufimtsev, I. S.; Martínez, T. J. Quantum Chemistry on Graphical Processing Units. 1. Strategies for Two-Electron Integral Evaluation. *J. Chem. Theory Comput.* **2008**, *4*, 222−231.
(21) Ufimtsev, I. S.; Martínez, T. J. Quantum Chemistry on Graphical Processing Units. 2. Direct Self-Consistent-Field Implementation. *J. Chem. Theory Comput.* **2009**, *5*, 1004−1015.
(22) Ufimtsev, I. S.; Martínez, T. J. Quantum Chemistry on Graphical Processing Units. 3. Analytical Energy Gradients, Geometry Optimization, and First Principles Molecular Dynamics. *J. Chem. Theory Comput.* **2009**, *5*, 2619−2628.
(23) DePrince, A. E.; Hammond, J. R. Coupled Cluster Theory on Graphics Processing Units I. The Coupled Cluster Doubles Method. *J. Chem. Theory Comput.* **2011**, *7*, 1287−1295.
(24) DePrince, A. E.; Kennedy, M. R.; Sumpter, B. G.; Sherrill, C. David Density-Fitted Singles and Doubles Coupled-Cluster on Graphics Processing Units. *Mol. Phys.* **2014**, *112*, 844−852.
(25) Eriksen, J. J. In *Parallel Programming with OpenACC*; Farber, R., Ed.; Morgan Kaufmann: 2017; p 241.
(26) Eriksen, J. J. Efficient and Portable Acceleration of Quantum Chemical Many-Body Methods in Mixed Floating Point Precision Using OpenACC Compiler Directives. *Mol. Phys.* **2017**, *115*, 2086−2101.
(27) Asadchev, A.; Gordon, M. S. Mixed-Precision Evaluation of Two-Electron Integrals by Rys Quadrature. *Comput. Phys. Commun.* **2012**, *183*, 1563−1567.
(28) Rák, Á.; Cserey, G. The BRUSH Algorithm for Two-Electron Integrals on GPU. *Chem. Phys. Lett.* **2015**, *622*, 92−98.
(29) Luehr, N.; Ufimtsev, I. S.; Martínez, T. J. Dynamic Precision For Electron Repulsion Integral Evaluation on Graphical Processing Units (GPUs). *J. Chem. Theory Comput.* **2011**, *7*, 949−954.
(30) Vogt, L.; Olivares-Amaya, R.; Kermes, S.; Shao, Y.; Amador-Bedolla, C.; Aspuru-Guzik, A. Accelerating Resolution-of-the-Identity Second-Order Möller-Plesset Quantum Chemistry Calculations with Graphical Processing Units. *J. Phys. Chem. A* **2008**, *112*, 2049−2057.
(31) Vysotskiy, V. P.; Cederbaum, L. S. Accurate Quantum Chemistry in Single Precision Arithmetic: Correlation Energy. *J. Chem. Theory Comput.* **2011**, *7*, 320−326.
(32) Knizia, G.; Li, W.; Simon, S.; Werner, H.-J. Determining the Numerical Stability of Quantum Chemistry Algorithms. *J. Chem. Theory Comput.* **2011**, *7*, 2387−2398.
(33) The metric for the amplitude convergence is the norm of the difference between the amplitudes from the successive iterations, i.e., $\|T^{(i)}-T^{(i-1)}\|$.
(34) The actual metric used in Molpro is the square of the norm of the difference between the amplitudes from the successive iterations, with the respective default threshold of $10^{-10}$.
(35) The metric for the amplitude convergence in GAMESS is the absolute value of the largest element of the difference between the amplitudes from the successive iterations, i.e., $\max|T^{(i)}-T^{(i-1)}|$.
(36) Epifanovsky, E.; Wormit, M.; Kuś, T.; Landau, A.; Zuev, D.; Khistyaev, K.; Manohar, P. U.; Kaliman, I.; Dreuw, A.; Krylov, A. I. New Implementation of High-Level Correlated Methods Using a General Block-Tensor Library for High-Performance Electronic Structure Calculations. *J. Comput. Chem.* **2013**, *34*, 2293−2309.
(37) Kaliman, I.; Krylov, A. I. New Algorithm for Tensor Contractions on Multi-Core CPUs, GPUs, and Accelerators Enables CCSD and EOM-CCSD Calculations with over 1000 Basis Functions on a Single Compute Node. *J. Comput. Chem.* **2017**, *38*, 842−853.
(38) Krylov, A. I.; Gill, P. M. W. Q-Chem: An Engine for Innovation. *WIREs Comput. Mol. Sci.* **2013**, *3*, 317−326.
(39) Shao, Y.; Gan, Z.; Epifanovsky, E.; Gilbert, A. T. B.; Wormit, M.; Kussmann, J.; Lange, A. W.; Behn, A.; Deng, J.; Feng, X.; Ghosh, D.; Goldey, M.; Horn, P. R.; Jacobson, L. D.; Kaliman, I.; Khaliullin, R. Z.; Kus, T.; Landau, A.; Liu, J.; Proynov, E. I.; Rhee, Y. M.; Richard, R. M.; Rohrdanz, M. A.; Steele, R. P.; Sundstrom, E. J.; Woodcock, H. L., III; Zimmerman, P. M.; Zuev, D.; Albrecht, B.; Alguires, E.; Austin, B.; Beran, G. J. O.; Bernard, Y. A.; Berquist, E.; Brandhorst, K.; Bravaya, K. B.; Brown, S. T.; Casanova, D.; Chang, C.-M.; Chen, Y.; Chien, S. H.; Closser, K. D.; Crittenden, D. L.; Diedenhofen, M.; DiStasio, R. A., Jr.; Do, H.; Dutoi, A. D.; Edgar, R. G.; Fatehi, S.; Fusti-Molnar, L.; Ghysels, A.; Golubeva-Zadorozhnaya, A.; Gomes, J.; Hanson-Heine, M. W. D.; Harbach, P. H. P.; Hauser,


DOI: 10.1021/acs.jctc.8b00321
J. Chem. Theory Comput. 2018, 14, 4088−4096

A. W.; Hohenstein, E. G.; Holden, Z. C.; Jagau, T.-C.; Ji, H.; Kaduk, B.; Khistyaev, K.; Kim, J.; Kim, J.; King, R. A.; Klunzinger, P.; Kosenkov, D.; Kowalczyk, T.; Krauter, C. M.; Laog, K. U.; Laurent, A.; Lawler, K. V.; Levchenko, S. V.; Lin, C. Y.; Liu, F.; Livshits, E.; Lochan, R. C.; Luenser, A.; Manohar, P.; Manzer, S. F.; Mao, S.-P.; Mardirossian, N.; Marenich, A. V.; Maurer, S. A.; Mayhall, N. J.; Oana, C. M.; Olivares-Amaya, R.; O'Neill, D. P.; Parkhill, J. A.; Perrine, T. M.; Peverati, R.; Pieniazek, P. A.; Prociuk, A.; Rehn, D. R.; Rosta, E.; Russ, N. J.; Sergueev, N.; Sharada, S. M.; Sharmaa, S.; Small, D. W.; Sodt, A.; Stein, T.; Stuck, D.; Su, Y.-C.; Thom, A. J. W.; Tsuchimochi, T.; Vogt, L.; Vydrov, O.; Wang, T.; Watson, M. A.; Wenzel, J.; White, A.; Williams, C. F.; Vanovschi, V.; Yeganeh, S.; Yost, S. R.; You, Z.-Q.; Zhang, I. Y.; Zhang, X.; Zhou, Y.; Brooks, B. R.; Chan, G. K. L.; Chipman, D. M.; Cramer, C. J.; Goddard, W. A., III; Gordon, M. S.; Hehre, W. J.; Klamt, A.; Schaefer, H. F., III; Schmidt, M. W.; Sherrill, C. D.; Truhlar, D. G.; Warshel, A.; Xu, X.; Aspuru-Guzik, A.; Baer, R.; Bell, A. T.; Besley, N. A.; Chai, J.-D.; Dreuw, A.; Dunietz, B. D.; Furlani, T. R.; Gwaltney, S. R.; Hsu, C.-P.; Jung, Y.; Kong, J.; Lambrecht, D. S.; Liang, W. Z.; Ochsenfeld, C.; Rassolov, V. A.; Slipchenko, L. V.; Subotnik, J. E.; van Voorhis, T.; Herbert, J. M.; Krylov, A. I.; Gill, P. M. W.; Head-Gordon, M. Advances in molecular quantum chemistry contained in the Q-Chem 4 program package. *Mol. Phys.* **2015**, *113*, 184−215.

(40) Jagau, T.-C.; Bravaya, K. B.; Krylov, A. I. Extending Quantum Chemistry of Bound States to Electronic Resonances. *Annu. Rev. Phys. Chem.* **2017**, *68*, 525−553.

(41) Dreuw, A.; Wormit, M. The Algebraic Diagrammatic Construction Scheme for the Polarization Propagator for the Calculation of Excited States. *WIREs Comput. Mol. Sci.* **2015**, *5*, 82−95.

(42) Ibrahim, K. Z.; Epifanovsky, E.; Williams, S.; Krylov, A. I. Cross-Scale Efficient Tensor Contractions for Coupled Cluster Computations Through Multiple Programming Model Backends. *J. Parallel Distrib. Comput.* **2017**, *106*, 92−105.

(43) The templated libtensor code enabling both single- and double-precision calculations is available in the *sp* branch at https://github.com/epifanovsky/libtensor.

(44) Levchenko, S. V.; Krylov, A. I. Equation-of-Motion Spin-Flip Coupled-Cluster Model with Single and Double Substitutions: Theory and Application to Cyclobutadiene. *J. Chem. Phys.* **2004**, *120*, 175−185.

(45) Curtiss, L. A.; Raghavachari, K.; Pople, J. A. Assessment of Gaussian-2 and Density Functional Theories for the Computation of Enthalpies of Formation. *J. Chem. Phys.* **1997**, *106*, 1063−1079.

(46) The metric for the EOM amplitude convergence is the norm of the residual vector, $\| \bar{H}R_k - \omega_k R_k \|$, where $R_k$ and $\omega_k$ are EOM amplitudes and energies at a given iteration.

(47) Krylov, A. I. The Spin-Flip Equation-of-Motion Coupled-Cluster Electronic Structure Method for a Description of Excited States, Bond-Breaking, Diradicals, and Driradicals. *Acc. Chem. Res.* **2006**, *39*, 83−91.

(48) Slipchenko, L. V.; Krylov, A. I. Singlet-Triplet Gaps in Diradicals by the Spin-Flip Approach: A Benchmark Study. *J. Chem. Phys.* **2002**, *117*, 4694−4708.

(49) Sattelmeyer, K. W.; Schaefer, H. F.; Stanton, J. F. Use of 2h and 3h-p Like Coupled-Cluster Tamm-Dancoff Approaches for the Equilibrium Properties of Ozone. *Chem. Phys. Lett.* **2003**, *378*, 42−46.

(50) O'Boyle, N. M.; Banck, M.; James, C. A.; Morley, C.; Vandermeersch, T.; Hutchison, G. R. Open Babel: An Open Chemical Toolbox. *J. Cheminf.* **2011**, *3*, 33.



DOI: 10.1021/acs.jctc.8b00321
*J. Chem. Theory Comput.* 2018, 14, 4088−4096